

# Identifying topological order by entanglement entropy

Hong-Chen Jiang<sup>1</sup>, Zhenghan Wang<sup>2</sup> and Leon Balents<sup>1\*</sup>

**Topological phases are unique states of matter that incorporate long-range quantum entanglement and host exotic excitations with fractional quantum statistics. Here we report a practical method to identify topological phases in arbitrary realistic models by accurately calculating the topological entanglement entropy using the density matrix renormalization group (DMRG). We argue that the DMRG algorithm systematically selects a minimally entangled state from the quasi-degenerate ground states in a topological phase. This tendency explains both the success of our method and the absence of ground-state degeneracy in previous DMRG studies of topological phases. We demonstrate the effectiveness of our procedure by obtaining the topological entanglement entropy for several microscopic models, with an accuracy of the order of  $10^{-3}$ , when the circumference of the cylinder is around ten times the correlation length. As an example, we definitively show that the ground state of the quantum  $S = 1/2$  antiferromagnet on the kagome lattice is a topological spin liquid, and strongly constrain the conditions for identification of this phase of matter.**

Theory has shown that quantum ground states may exhibit distinct patterns of long-range entanglement, which provides the most basic categorization of quantum phases of matter, more fundamental than Landau's symmetry-breaking paradigm. The simplest and most robust long-range entangled states, which have a full spectral gap, comprise topological phases, which host topological order. Much recent interest in topological phases is due to the prospect of using them to construct an inherently fault-tolerant quantum computer<sup>1,2</sup>. Topological phases are also of basic scientific interest for their many unique properties, especially their ability to support exotic excitations with fractional and even non-Abelian quantum statistics.

Crystalline Mott insulators with unpaired electron spins have long been considered likely candidates for long-range entangled states, epitomized in this context by Anderson's resonating-valence-bond<sup>3</sup> wavefunction for a quantum spin liquid<sup>4</sup>. As this particular state is non-magnetic, the lack of magnetic order has been widely taken as a definition of a quantum spin liquid. However, defining what a quantum spin liquid is not has little utility, and is especially unhelpful in the theoretical search for these phases. Instead, a positive definition of a quantum spin liquid that can be tractably tested in realistic models is sorely needed.

In principle, such a positive definition is provided for topological phases (and hence those quantum spin liquids with topological order) by the topological entanglement entropy (TEE) introduced by Kitaev and Preskill<sup>5</sup> and Levin and Wen<sup>6</sup>. Unfortunately, the formulations in refs 5,6 suffer from severe finite-size corrections due to lattice-scale effects, greatly hindering their application. We report here a practical and extremely simple scheme to numerically calculate the TEE, and thereby identify topological order. Our method consists simply of using the DMRG<sup>7,8</sup> to calculate the usual entanglement entropy for the division of a cylinder into two equal halves by a flat cut, and extracting the TEE from its asymptotic, large-circumference limit. We argue that this method actually works, despite potential complications known theoretically<sup>9,10</sup>, owing to a subtle ground-state selection mechanism built into

the DMRG algorithm. The approach is tested here on a variety of lattice models, and then applied successfully to the physically realistic quantum spin  $S = 1/2$  anti-ferromagnetic Heisenberg  $J_1$ - $J_2$  model on the kagome lattice. By extracting an accurate TEE, we identify a quantum spin-liquid state with topological order for the first time in a physically realistic  $SU(2)$ -invariant lattice model. We emphasize that the TEE provides positive, smoking-gun evidence for a topological quantum spin liquid, and excludes any topologically trivial states, regardless of possible complex or subtle broken symmetries. The value of the TEE also greatly restricts the possible topological quantum field theories that fully describe the topological order. We return to this at the end of this paper.

The TEE is derived from the bipartite von Neumann entanglement entropy, which is defined by dividing a system into two subsystems, A and B, which together constitute or make up the full system. The entanglement entropy associated with this partition is defined from the reduced density matrix,  $\rho_A = \text{Tr}(|0\rangle\langle 0|)$ , where  $|0\rangle$  is a ground state, according to  $S(A) = -\text{Tr}(\rho_A \ln(\rho_A))$ . It has the duality property  $S(A) = S(B)$ . According to the seminal works of Kitaev and Preskill<sup>5</sup> and Levin and Wen<sup>6</sup>, the entanglement entropy of a partition of a two-dimensional system where A is a disc-like region with a smooth boundary (the entanglement surface) of length  $\ell$  scales as

$$S(A) = \alpha\ell - \gamma + \dots \quad (1)$$

where the ellipsis represents terms that vanish in the limit  $\ell \rightarrow \infty$ . The coefficient  $\alpha$ , owing to short-distance physics near the boundary, is non-universal. The term  $\gamma$  is the TEE—a universal additive constant characterizing the long-range entanglement in the ground state that can be quantified as  $\gamma = \ln D$ , where  $D$  is the total quantum dimension of the medium<sup>5,6</sup>.

Note that  $\gamma$  is sub-dominant to the  $\alpha\ell$  term, arising from short-range entanglement. As a consequence, it is non-trivial to extract. Moreover, for real lattice systems, it is not obvious how to

<sup>1</sup>Kavli Institute for Theoretical Physics, University of California, Santa Barbara, California 93106, USA, <sup>2</sup>Microsoft Station Q, University of California, Santa Barbara, California 93106, USA. \*e-mail: balents@kitp.ucsb.edu.

define  $\ell$  on the lattice, nor is it obvious what qualifies as a smooth boundary. These two ambiguities are particularly challenging.

In refs 5,6, complex prescriptions were proposed to remove the short-range contributions and extract the TEE from measurements on planar partitions. In our much simpler scheme, we study a single partition, defined by a straight cut normal to a cylinder that divides it in half, and extract the TEE using equation (1) with  $\ell = L_y$ , the circumference of the cylinder. This approach minimizes errors due to subtractions of many large numbers, and also minimizes finite-size corrections due to short-range entanglement, as we now argue.

For the cylindrical case, we expect such finite-size corrections to be of the order of  $e^{-L_y/\xi}$ . In the Kitaev–Preskill and Levin–Wen formulations, the corrections are much larger. There, to obtain the TEE, the entropy is calculated for several disc-like planar partitions, and corner contributions are cancelled by forming a linear combination of the results. However, the complicated shape of the planar partitions involved means that the smallest spatial features of the partition are several times smaller than the overall system width. For instance, in the Levin–Wen formulation, the smallest features (size  $d$ ) are at least four times smaller than the linear width of the system assuming periodic boundary conditions, so that  $L \geq 4d$ , a conservative estimate. Corrections to equation (1) should be expected to be of the order of  $e^{-d/\xi} \geq e^{-L/(4\xi)}$ . Thus, to obtain a similar performance to that of the cylindrical cut, even assuming no additional errors are introduced by the subtractions of different entropies, requires a linear system size at least four times larger in the Levin–Wen case. This means at least 16 times as many spins, and given the exponential growth of the Hilbert space with the number of quantum degrees of freedom, this is a very costly increase. Indeed, attempts to implement the Kitaev–Preskill and Levin–Wen protocols in simulations have shown them to be very challenging numerically<sup>11,12</sup>.

A potential complication of our method is that the ground state on a cylinder is expected to have a degeneracy in a topological phase in the thermodynamic limit, and the TEE for the cylindrical cut can depend on which ground state the TEE is measured in refs 9 and 10. In ref. 10, it has been shown, however, that the TEE for the  $\mathbb{Z}_2$  spin liquid is bounded above by the universal value  $\gamma = \ln 2$ , and below by zero. Moreover, in general the universal value is achieved for so-called minimal entropy states<sup>10</sup> (MESs), which correspond to states in which a quasiparticle is definitely contained within the region A (or B). For the  $\mathbb{Z}_2$  spin liquid, the MESs are the states with a definite  $\mathbb{Z}_2$  magnetic flux through the cylinder, that is, the vison or no-vison eigenstates.

We suggest, on the basis of numerical evidence, that the DMRG systematically finds a MES. This is perhaps natural because the DMRG prefers low-entanglement states<sup>8</sup>. Note though that the absolute ground state of a finite system is dependent on microscopic details, and is expected to vary with the aspect ratio ( $L_x/L_y$ ) of the cylinder<sup>13</sup>. For a physical Hamiltonian without fine-tuning, the absolute ground state becomes a MES in the long-cylinder limit, where  $L_x/L_y$  is larger than some critical value (which depends on microscopic details, but is the order of 1 generically)<sup>13</sup>. However, we contend that the DMRG preferentially finds the MES even when it is not the absolute ground state. Evidence for this is given below in the toric-code model, where the MES can be explicitly identified. The fact that we obtain the universal value of the TEE, independent of the system’s aspect ratio, for several other models, also supports this conclusion.

We turn now to the toric-code model, which is well known—see the Supplementary Information for details of the definition. It can be considered as a model of fluctuating discrete electric and magnetic fields. To observe the ground-state selection, we first consider an applied field  $h = h_x \neq 0$  that is purely electric,  $h_z = 0$ . In this non-generic model the absolute ground state is demonstrably not a MES. Specifically, the operator  $G$  (defined in the

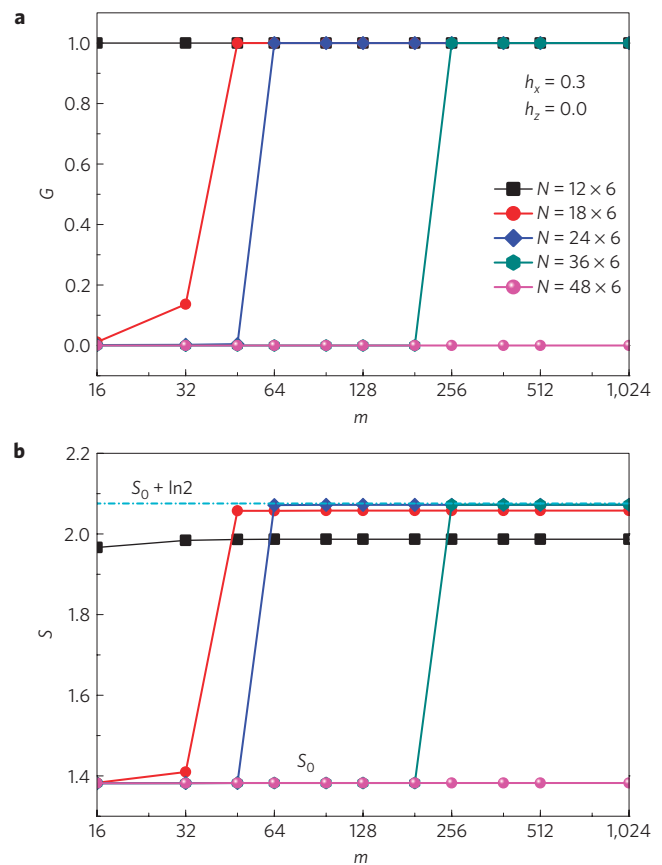


**Figure 1 | Evidence that the DMRG favours MESs. a,b**, The electric field parity ( $G$ ) (**a**) and the entanglement entropy (**b**) versus the number of states  $m$  for the toric code with  $h_x = 0.3$  and  $h_z = 0.0$ , for several system sizes (colour key in **a** applies to both). For a fixed small system size, at smaller  $m$  the average parity  $\langle G \rangle$  is approximately zero and the entanglement is reduced, whereas at large  $m$  a definite parity eigenstate is found with  $G = 1$ , and the entanglement is increased. The jumps in the two quantities coincide, signalling a transition from a MES to an absolute Hamiltonian eigenstate. The number of states  $m$  needed to converge to the absolute ground state increases rapidly with  $L_x$ . For larger systems than shown, a MES with  $\langle G \rangle \approx 0$  is found for all accessible values of  $m$ .

Supplementary Material), which measures the parity of the number of electric-field loops winding around the cylinder, commutes with the Hamiltonian, so the energy eigenstates must also be eigenstates of  $G = \pm 1$ . Topological order implies that there are two such states with  $G = +1$  and  $G = -1$ , with exponentially close energies. The MESs, however, are not  $G$  (or energy) eigenstates, but rather the superpositions  $|\pm\rangle = (|G = 1\rangle \pm |G = -1\rangle)/\sqrt{2}$ , for which  $\langle \pm | G | \pm \rangle = 0$ . The  $|\pm\rangle$  states correspond to states with or without magnetic flux through the cylinder. Measurements of  $\langle G \rangle$  and  $S$  (Fig. 1) show that the DMRG preferentially selects a MES for larger systems, and that the number of states  $m$  necessary to converge to the absolute ground state (with larger entanglement and zero TEE—see Fig. 2b) grows very rapidly with system size.

The origin of the topological contributions to the entanglement entropy sheds light on this behaviour in the  $\mathbb{Z}_2$  case of interest. First, there is a reduction of entropy due to the constraint that electric-field loops always cross the entanglement surface an even number of times. This reduction is precisely the TEE, and this physics is included once entanglement on the scale of  $L_y$  is taken into account. Second, in the case where the absolute ground state is not a MES, there is an increase of entropy due to the global constraint on the number of electric-field lines winding

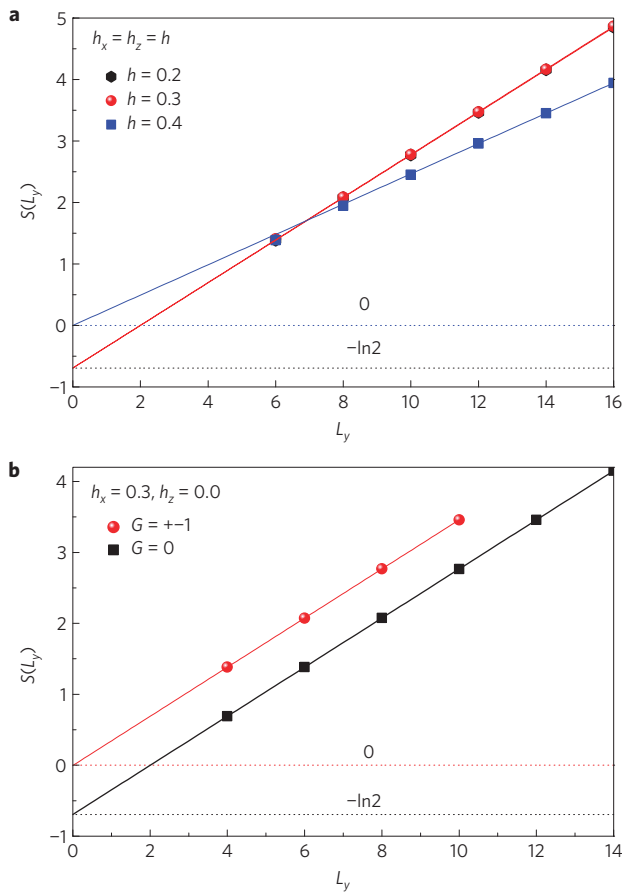


**Figure 2 | The von Neumann entropy  $S(L_y)$  for the toric-code model in magnetic fields.** **a**,  $S(L_y)$  with  $L_y = 4\text{--}16$  at  $L_x = \infty$  for symmetric magnetic fields at  $h_x = h_z = h = 0.2, 0.3$  and  $0.4$ . By fitting  $S(L_y) = aL_y - \gamma$ , we get  $\gamma = 0.693(1), 0.691(4)$  and  $0.001(5)$ , respectively. **b**, The pure electric case,  $h_x = 0.3, h_z = 0$ , and comparison of  $S(L_y)$  in the MES obtained in the large  $L_x$  limit (black squares) with that of the absolute ground state from systems of dimensions  $L_x \times L_y = 20 \times 4, 24 \times 6, 24 \times 8, 24 \times 10$  (red circles). Extrapolation shows that the MES has the universal TEE, whereas the absolute ground state has zero TEE.

around the entire cylinder. To take this into account, the DMRG must fully converge the entanglement of the opposite ends of the system, which are extremely far apart on the snaking DMRG path. This global entanglement does not converge for larger systems, in which case the DMRG produces states described by a Schmidt decomposition in which the left and right halves of the system have uncorrelated electric-field winding parities. Such a state is a MES.

We next consider the toric-code model in symmetrically applied fields,  $h_x = h_z = h$ , for which the absolute ground state is not obvious. Figure 2 shows the entanglement entropy in this case. This model was previously shown<sup>14</sup> to have a quantum phase transition between the  $\mathbb{Z}_2$  phase for  $h < h_c \approx 0.34$  and a trivial phase for  $h > h_c$ . The extrapolated TEE following our protocol indeed very well approximates the universal value  $\gamma = \ln 2 = 0.69314\dots$  for  $h < h_c$ ; even for  $h = 0.3$ , relatively close to the quantum phase transition, we obtain  $\gamma = 0.691(4)$ , which is accurate to a fraction of a per cent. For  $h > h_c$ , we obtain  $\gamma = 0$ , as expected, with a numerical uncertainty of the order of  $10^{-3}$ . Similar results are obtained for a variety of aspect ratios and values of the perturbing fields.

We apply the method to the spin-1/2 Heisenberg model on the kagome lattice, for which compelling but indirect evidence for a gapped quantum spin liquid has recently been obtained by extensive DMRG studies<sup>15–17</sup>. We consider the model with both first- and

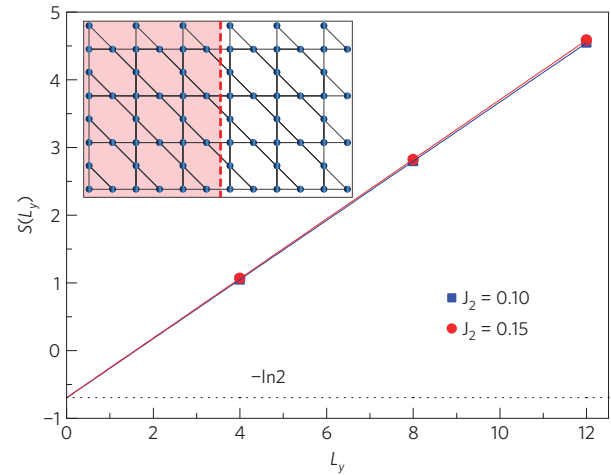


**Figure 3 | The entanglement entropy  $S(L_y)$  of the kagome  $J_1$ – $J_2$  model in equation (2), with  $L_y = 4\text{--}12$  at  $L_x = \infty$ . By fitting  $S(L_y) = aL_y - \gamma$ , we get  $\gamma = 0.698(8)$  at  $J_2 = 0.10$  and  $\gamma = 0.694(6)$  at  $J_2 = 0.15$ . Inset: kagome lattice with  $L_x = 12$  and  $L_y = 8$ .**

second-neighbour interactions, whose Hamiltonian is

$$H = J_1 \sum_{\langle ij \rangle} \mathbf{S}_i \cdot \mathbf{S}_j + J_2 \sum_{\langle\langle ij \rangle\rangle} \mathbf{S}_i \cdot \mathbf{S}_j \quad (2)$$

where  $\mathbf{S}_i$  is the spin operator on site  $i$ , and  $\langle ij \rangle$  ( $\langle\langle ij \rangle\rangle$ ) denotes the nearest neighbours (next-nearest neighbours). In the numerical simulation, we set  $J_1 = 1$  as the unit of energy. The most recent DMRG studies<sup>17</sup> show that the  $J_2 = 0$  point is near the edge of a substantial spin-liquid phase centred near  $J_2 = 0.05\text{--}0.15$ .

We take the kagome lattice with periodic boundary conditions along a bond direction, drawn vertically in the inset of Fig. 3, and the unit of length equal to the nearest-neighbour distance. The results for the entanglement entropy for  $J_2 = 0.10$  and  $0.15$  are shown in Fig. 3 with a correlation length of around one-lattice spacing for both spin–spin and dimer–dimer correlation functions. We see that a linear fit using data for  $L_y = 4 \sim 12$  using equation (1) gives  $\gamma = 0.698(8)$  at  $J_2 = 0.10$  and  $\gamma = 0.694(6)$  at  $J_2 = 0.15$ , both within one per cent of  $\ln 2 = 0.693$ . This proves definitively that this phase is a topological spin liquid, and determines the quantum dimension  $D = 2$ , consistent with a  $\mathbb{Z}_2$  state, which<sup>18,19</sup> was proposed for the kagome Heisenberg model without second-neighbour interactions, that is,  $J_2 = 0$ .

We have shown that the TEE can be calculated to an accuracy of the order of  $10^{-3}$  when  $L_y$  is  $\sim 10$  times the correlation length (see the Supplementary Material for some further tests). Our result provides a smoking-gun test for a topological spin liquid. It also explains the puzzling absence of topological degeneracy in recent DMRG results that otherwise support a  $\mathbb{Z}_2$  spin-liquid state<sup>13,16</sup>, because we have shown that the DMRG is systematically biased to find just one of the ground states. The TEE does not fully determine the nature of the topological phase. Fortunately, for a given  $D$ , there are only finitely many distinct topological phases, and for small values of  $D$ , a complete classification of all topological phases is known<sup>20</sup>. Other constraints such as time-reversal symmetry (if present) further constrain the possible topological order. For example, there are only two time-reversal-invariant phases consistent with  $D = 2$ , found here for the kagome Heisenberg model: the  $\mathbb{Z}_2$  phase and a doubled semion phase. It will be interesting to develop methods to distinguish these in the future, and to calculate the topological ground-state splitting. Identifying topological order by combining theoretical classification results with numerical simulation is a major step in the development of a post-Landau paradigm for classifying quantum phases of matter.

Note added in proof. After the submission of this paper, we became aware of a similar result published in a recent paper<sup>21</sup>.

Received 18 May 2012; accepted 28 September 2012;  
published online 11 November 2012

## References

1. Kitaev, A. Y. Fault-tolerant quantum computation by anyons. *Ann. Phys.* **303**, 2–30 (2003).
2. Nayak, C., Simon, S. H., Stern, A., Freedman, M. & Das Sarma, S. Non-abelian anyons and topological quantum computation. *Rev. Mod. Phys.* **80**, 1083–1159 (2008).
3. Anderson, P. W. Resonating valence bonds: A new kind of insulator? *Mater. Res. Bull.* **8**, 153–160 (1973).
4. Balents, L. Spin liquids in frustrated magnets. *Nature* **464**, 199–208 (2010).
5. Kitaev, A. & Preskill, J. Topological entanglement entropy. *Phys. Rev. Lett.* **96**, 110404 (2006).
6. Levin, M. & Wen, X.-G. Detecting topological order in a ground state wave function. *Phys. Rev. Lett.* **96**, 110405 (2006).
7. White, S. R. Density matrix formulation for quantum renormalization groups. *Phys. Rev. Lett.* **69**, 2863–2866 (1992).
8. Stoudenmire, E. M. & White, S. R. Studying two dimensional systems with the density matrix renormalization group. *Annu. Rev. Condens. Matter Phys.* **3**, 111–128 (2012).
9. Dong, S., Fradkin, E., Leigh, R. G. & Nowling, S. Topological entanglement entropy in Chern-Simons theories and quantum Hall fluids. *J. High Energy Phys.* **05**, 016 (2008).
10. Zhang, Y., Grover, T., Turner, A., Oshikawa, M. & Vishwanath, A. Quasiparticle statistics and braiding from ground-state entanglement. *Phys. Rev. B* **85**, 235151 (2012).
11. Furukawa, S. & Misguich, G. Topological entanglement entropy in the quantum dimer model on the triangular lattice. *Phys. Rev. B* **75**, 214407 (2007).
12. Isakov, S. V., Hastings, M. B. & Melko, R. G. Topological entanglement entropy of a Bose-Hubbard spin liquid. *Nature Phys.* **7**, 772–775 (2011).
13. Jiang, H. C., Yao, H. & Balents, L. Spin liquid ground state of the spin-1/2 square  $J_1$ - $J_2$  Heisenberg model. *Phys. Rev. B* **86**, 024424 (2012).
14. Trebst, S., Werner, P., Troyer, M., Shtengel, K. & Nayak, C. Breakdown of a topological phase: Quantum phase transition in a loop gas model with tension. *Phys. Rev. Lett.* **98**, 070602 (2007).
15. Jiang, H. C., Weng, Z. Y. & Sheng, D. N. Density matrix renormalization group numerical study of the kagome antiferromagnet. *Phys. Rev. Lett.* **101**, 117203 (2008).
16. Yan, S., Huse, D. & White, S. Spin-liquid ground state of the  $S = 1/2$  kagome Heisenberg antiferromagnet. *Science* **332**, 1173–1176 (2011).
17. White, S. R. The spin liquid ground state of the  $S = 1/2$  Heisenberg model on the kagome lattice. *Bull. Am. Phys. Soc.* **57** MAR.L19.1 (2012); available at <http://meetings.aps.org/link/BAPS.2012.MAR.L19.1>.
18. Wen, X. G. Mean-field theory of spin-liquid states with finite energy gap and topological orders. *Phys. Rev. B* **44**, 2664–2672 (1991).
19. Read, N. & Sachdev, S. Large- $N$  expansion for frustrated quantum antiferromagnets. *Phys. Rev. Lett.* **66**, 1773–1776 (1991).
20. Rowell, E., Stong, R. & Wang, Z. On classification of modular tensor categories. *Commun. Math. Phys.* **292**, 343–389 (2009).
21. Depenbrock, S., McCulloch, I. P. & Schollwoeck, U. Nature of the spin-liquid ground state of the  $S = 1/2$  Heisenberg model on the Kagome lattice. *Phys. Rev. Lett.* **109**, 067201 (2012).

## Acknowledgements

We thank T. Grover and A. Vishwanath for a helpful explanation of their work, and S. White for helpful discussions. H.C.J. thanks H. Yao for collaboration on related projects. This work was supported by the NSF through grant DMR 0804564 (L.B.), the NSF MRSEC Program under DMR 1121053, the NBRPC (973 Program) 2011CBA00300 (2011CBA00302), and benefited from the facilities of the KITP, supported by NSF PHY05-51164.

## Author contributions

H.C.J. developed the simulation codes and performed the numerical experiments. All authors were equally responsible for writing the manuscript.

## Additional information

Supplementary information is available in the online version of the paper. Reprints and permissions information is available online at [www.nature.com/reprints](http://www.nature.com/reprints). Correspondence and requests for materials should be addressed to L.B.

## Competing financial interests

The authors declare no competing financial interests.